Supplementary Information

Stiffness of fluid and gel phase lipid nanovesicles: weighting the contributions of membrane bending modulus and luminal pressurization

Andrea Ridolfi [a,b,c,], Lucrezia Caselli [a,c], Matteo Baldoni [b], Costanza Montis [a,c], Francesco Mercuri [b], Debora Berti [a,c], Francesco Valle [a,b,*] and Marco Brucale [a,b,*].*

[a] Consorzio Interuniversitario per lo Sviluppo dei Sistemi a Grande Interfase, 50019 Firenze, Italy.

[b] Consiglio Nazionale delle Ricerche, Istituto per lo Studio dei Materiali Nanostrutturati, 40129 Bologna, Italy.

[c] Dipartimento di Chimica "Ugo Schiff", Università degli Studi di Firenze, 50019 Firenze, Italy.

** corresponding authors*

Figure S1

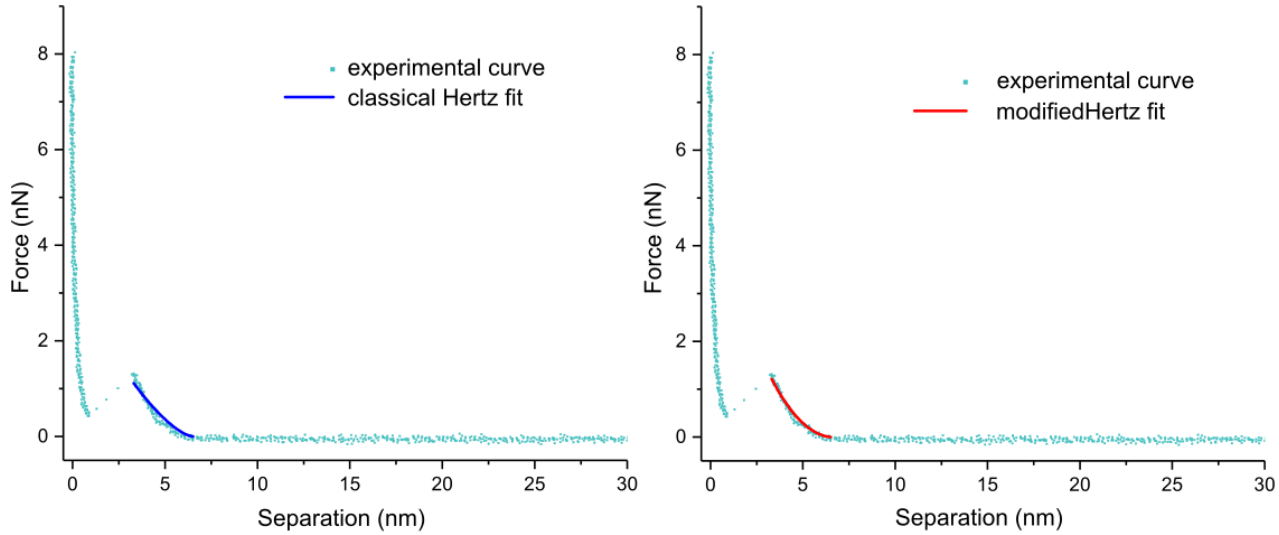

Difference between the classical and the corrected Hertz fitting model (proposed by Dimitriadis et al.); as can be seen, the classical Hertz fit underestimates the Young Modulus, indeed the fitted curve is less steep than the original one. On the other hand, the modified Hertz fit presents a much better accord with the experimental data. This is probably due to the low thickness of the lipid bilayers and to the related substrate contributions; both being phenomena not taken under sufficient consideration by the Hertz theory. The more recent model, proposed by Dimitriadis et al. (1) instead, accounts for those cases in which the substrate contributions become relevant, as a consequence of the low layer thickness.

Additional details about the particle-based molecular dynamics (MD) simulations

The support surface was composed by seven stacked layers of SGA beads arranged in a hexagonal (honeycomb) lattice, with a 2:1 mapping with respect to graphite. The interaction within the particles constituting the support layer was defined in terms of a deep LJ potential only. This allows to exclude the mechanical part of the potential from the total energy. The interaction of the support layer with all other particles was defined by using the parameters of SN0 beads. The surface roughness was introduced by randomly removing a variable number of particles from the support layers, from 90%

for the topmost layer to 0% in the central layer. A model substrate of about 30x30 nm with periodicity in 2 dimensions was first relaxed by MD in vacuum.

The model system constituted by the SLB model in water solution and the AFM tip model, at a distance of about 8 nm from the surface, was first relaxed by equilibrium MD for about 40 ns in the NPT ensemble, keeping the particle of the AFM tip fixed (see also Fig. S2).

From this initial run, configurations were extracted at intervals of 0.75 nm along the trajectory. These configurations were used as starting points for equilibrium MD simulations (about 50 ns), keeping the AFM tip model fixed and evaluating the mean force between the tip and the SLB over the last 5 ns.

Figure S2

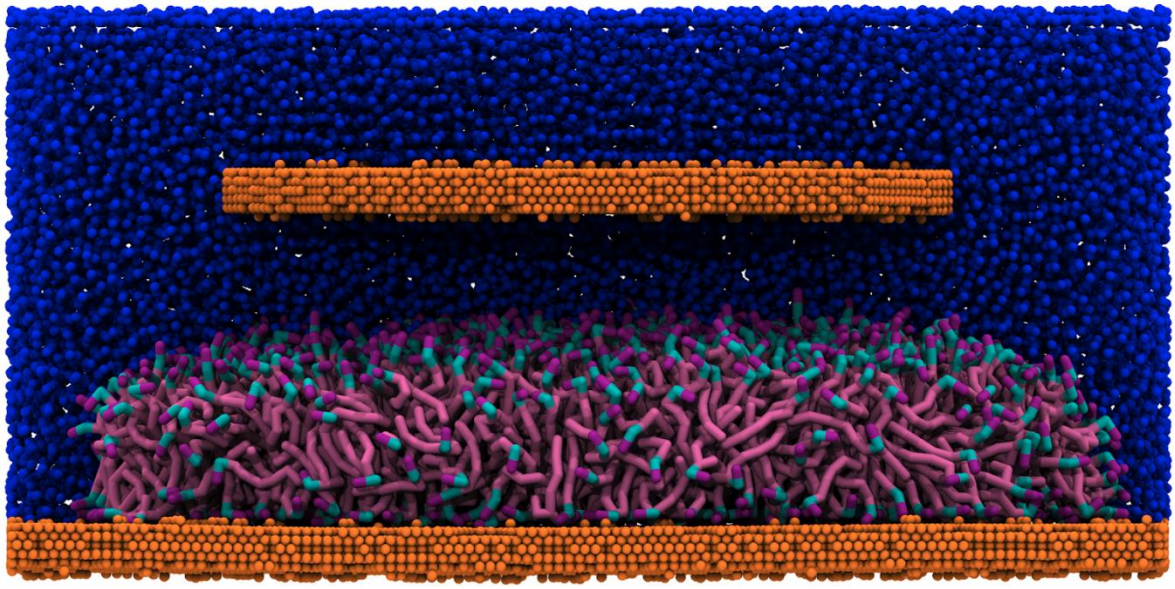

Side view (section) of the model system used in MD simulations of a DPPC SLB. Particles of the support layer (bottom) and of the mechanical probe (top) are in orange; water particles are in blue. The lateral size of the model shown is 30 nm. The figure shows a snapshot from one of the equilibration runs carried out to evaluate the force between the mechanical probe and the SLB

Figure S3

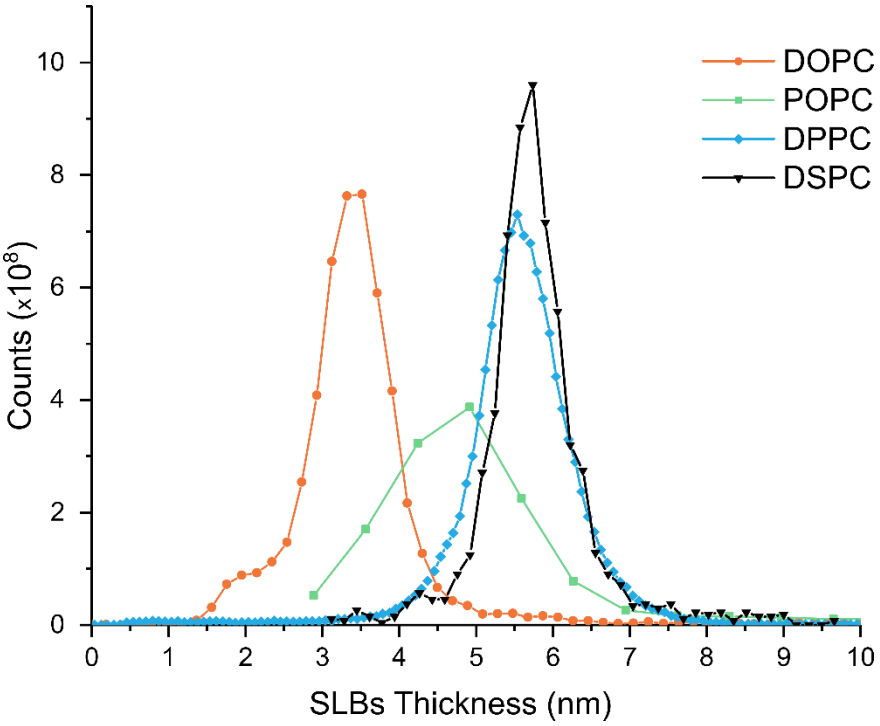

AFM images of SLBs were analyzed and processed using Gwyddion(2), following the procedures described elsewhere(3), in order to extract the height distributions of the SLBs from the four different lipid types. Peaks of the distributions were then fitted to obtain an average value of the SLB thickness. Numerical results from the fits are displayed in Table S1.

Figure S4

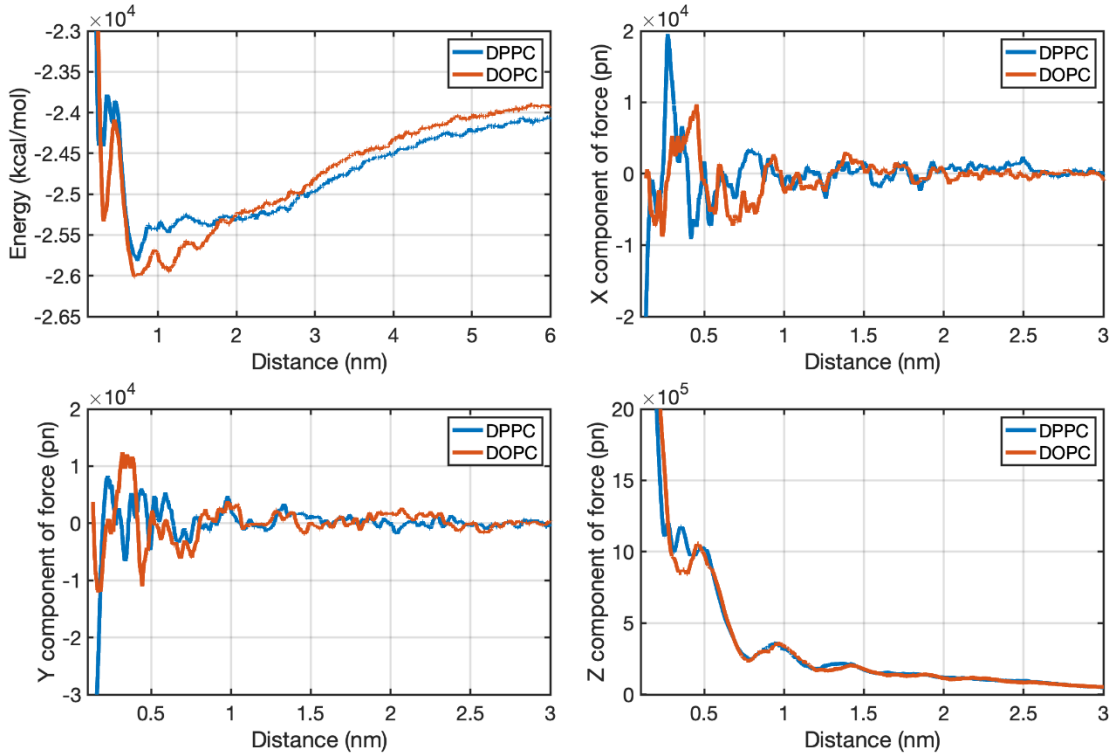

Total energy and components of the force between the mechanical probe model and the SLB for the initial (non-equilibrium) trajectories. DPPC: blue curves; DOPC: orange curves.

Table S1:

Thickness values of the different Supported Lipid Bilayers obtained by fitting the distributions of Figure S4; the indicated thicknesses refer to the position of the maxima in the plots, i.e., the most counted thickness values.

Lipid	SLB thickness (nm)
DOPC	3.70 ± 0.36
POPC	4.32 ± 0.53
DPPC	5.58 ± 0.42
DSPC	5.67 ± 0.55

Table S2:

Curvature radii of the liposomes measured in this study; at least 15 vesicles for each lipid were measured via AFM-FS. The curvature radius (R_c) of each vesicle was measured by fitting the profile of the adsorbed vesicle, using Gwyddion(2). Mean curvature radii and their standard deviations are also reported below.

DOPC	R_c (nm)	POPC	R_c (nm)	DPPC	R_c (nm)	DSPC	R_c (nm)
Vesicle 1	80.7	Vesicle 1	84.2	Vesicle 1	80.7	Vesicle 1	81.7
Vesicle 2	84.3	Vesicle 2	115.6	Vesicle 2	105.5	Vesicle 2	58.2
Vesicle 3	116.8	Vesicle 3	104.2	Vesicle 3	94.7	Vesicle 3	40.8
Vesicle 4	84.1	Vesicle 4	72.4	Vesicle 4	191.8	Vesicle 4	81.6
Vesicle 5	78.0	Vesicle 5	19.5	Vesicle 5	156.6	Vesicle 5	36.1
Vesicle 6	80.3	Vesicle 6	33.2	Vesicle 6	72.8	Vesicle 6	49.4
Vesicle 7	46.4	Vesicle 7	89.6	Vesicle 7	49.6	Vesicle 7	62.0
Vesicle 8	102.8	Vesicle 8	52.2	Vesicle 8	68.1	Vesicle 8	44.3
Vesicle 9	53.3	Vesicle 9	38.5	Vesicle 9	57.3	Vesicle 9	52.1
Vesicle 10	57.1	Vesicle 10	39.1	Vesicle 10	45.1	Vesicle 10	73.5
Vesicle 11	76.1	Vesicle 11	49.5	Vesicle 11	30.8	Vesicle 11	54.3
Vesicle 12	74.4	Vesicle 12	59.9	Vesicle 12	34.9	Vesicle 12	89.4
Vesicle 13	91.5	Vesicle 13	61.1	Vesicle 13	47.4	Vesicle 13	103.7
Vesicle 14	76.7	Vesicle 14	37.7	Vesicle 14	51.5	Vesicle 14	81.5
Vesicle 15	90.6	Vesicle 15	53.3	Vesicle 15	35.5	Vesicle 15	79.0

Vesicle 16	65.3	Vesicle 16	60.8	Vesicle 16	49.3		
Vesicle 17	67.4	Vesicle 17	65.0	Vesicle 17	62.1		
Vesicle 18	68.5			Vesicle 18	71.8		
Vesicle 19	66.8			Vesicle 19	79.6		
Vesicle 20	77.7			Vesicle 20	39.7		
mean (nm)	76.9	**mean (nm)**	60.9	**mean (nm)**	71.2	**mean (nm)**	65.8
st. dev (nm)	16.4	**st. dev (nm)**	25.8	**st. dev (nm)**	40.9	**st. dev (nm)**	20.0